SIMULATING SILVER IODINE DISPERSION WITH WRF: HAIL SUPPRESSION SYSTEM ANALYSIS

Pablo G. Cremades[a,b]**, David G. Allende**[a,b] **and Salvador E. Puliafito**[a,b]

[a]*Grupo de Estudios de la Atmósfera y el Ambiente, Universidad Tecnológica Nacional – Facultad Regional Mendoza, Rodriguez 273, M5502AJE,Mendoza, Argentina, pablocremades@gmail.com,*
http://www.frm.utn.edu.ar/geaa

[b]*Consejo Nacional de Investigaciones Científicas y Técnicas (CONICET)*

Keywords: Hail storm, WRF-Fire model, silver iodide flare dispersion.

Abstract. The aim of this article is to study silver iodine (AgI) dispersion in Mendoza using the Weather Research and Forcasting model (WRF). AgI is used to seed clouds in hail suppression systems. In particular, in Mendoza, cloud seeding is done through ground generators located in the western part of the province, were most storm cells form. The efficiency of this hail suppression system has not been scientifically proven. This paper provides a methodology to include AgI sources in WRF in order to study its dispersion in the atmosphere. Because of the physical characteristics of ground generators, they are modeled as area sources using the Fire module of WRF. This module has been design to simulate biomass burning. We show how to simulate AgI generators through definition of a special fuel behavior model to use with WRF-Fire. Through dispersion modeling it is possible to see if AgI reaches storm cells. Furthermore, with simulation results it is possible to choose the best location for ground AgI generators. This paper shows a first approach to simulation of hail suppression system currently working in Mendoza.

1   INTRODUCTION

The Province of Mendoza in western Argentina is worldwide known for its wine production and for being one the most hail-prone areas in the world (Sánchez et al. 2013; Mezher et al. 2012; García-Ortega et al. 2009). Annually an average of 10% of the agricultural production in the Mendoza Province is lost as a result of severe hailstorms, and approximately 20% of the agricultural area receives hail precipitation, according to the local Hail Suppression Program statistics (http://www.contingencias.mendoza.gov.ar/).

Operational hail suppression programs have been working in Mendoza since 1970. The objective of such programs is to lessen the economic impact of hailstorms on wine industry. Some initial efforts employed Russian technology and Silver Iodide (AgI) rockets, guided by tracking radar, to seed the high-reflectivity cores of incipient hailstorms (Makitov, 1999). Although rockets can seed with high space and time precision, the system requires restrict to air-traffic control and qualified staff for rockets lines maintenance.

Lately, cloud seeding has been done with airplanes and ground generators. The Hail Suppression Program System in Mendoza counts with four fully equipped airplanes that work with emphasis on seeding young growing elements, typically the major feeders to the severe hailstorms already in progress. The main advantage of this system is that the seeding occurs in the correct region at the correct time. The main limitations are that the continuous seeding is impossible, the heavy clouds limit the precision of the process in space and time and the need high qualification staff (Zipori et al. 2012).

Ground generators burn a mixture of Silver Iodide (AgI) and Acetone to produce a "smoke" that contains the seeding agent. This smoke is transported to supercooled parts of the clouds by convective air flow. The ground-based generator system requires low maintenance costs, low qualification of the staff who can work on a partial-time basis and none coordination of air traffic. However, since seeding material is widely dispersed, a large quantity can be deactivated if the seeding is not made at the proper place and time. In that sense, due to the high operational cost of the hail suppression program, there is a call for scientific evidence of its efficiency in reducing hail precipitation.

Evaluating the seeding effect can be done by means of physical and/or statistical evidence [see for example the work in Bruintjes (1999)]. Likewise, many numerical simulations on seeding effects were made and are still undergoing to assist seeding programs, not only in choosing the seeding sites, but also at identifying potential areas that will be affected by seeding (Li and Pitter, 1997; Lee et al. 2009). Xue et al. (2013) show efforts made to simulate the effects of cloud seeding. However, there are no works on ground seeding dispersion modeling.

In this context, the objectives of this work are to develop a method to simulate AgI dispersion with the Weather Research and Forecasting model (WRF: Skamarock et al. 2008) and see if AgI from ground generator emissions can reach storm cells. Secondarily, results from this study could lead to optimization of location of such generators.

We adapted the Weather Research and Forecasting model (WRF) coupled to the surface fire behavior model (WRF-Fire: Mandel et al. 2011) to represent this particular type of AgI source. With this tool there is an opportunity to provide new insights, and to contribute to the current cloud seeding program management in Mendoza.

2   MATERIAL AND METHODS

2.1 Study area and experimental setup

The province of Mendoza in Argentina has been identified as a hotspot of convection in the Southern Hemisphere. The cloud seeding program in Mendoza is based on the conceptual model of Alberta (Canada) and Colorado hailstorms (Browning and Foote, 1976). This type of operational hail suppression system has been long studied and applied [see for example (DeMott 1995; Guo et al. 2006; Silverman 2010; Zipori et al. 2012) among many others]. The effectiveness of the cloud seeding has been also evaluated considering the transport of AgI to the target areas (Bruintjes 1999; Zipori et al. 2012).

The operational seeding period goes from 15 October to 1 April and the program covers the three agricultural oases of Mendoza–San Martín in the North of the Province, Tunuyán in the center, and San Rafael in the South.

In order to perform the simulations, the study area was centered at -33.938ºS, -68.413ºW, where the formation and development of severe convective storms usually occurs and where the AgI ground generator net is located (see Figure 1). The modeling domain contains 50x50 grid points with a grid separation of 600 m. Even though it is recommended to downscale global meteorological data in small steps using the nested domains feature in WRF model, in this case we have setup only one domain, because of computational constraints. The top layer of the model was set up at 50 hPa with 39 vertical levels logarithmically separated, being levels near the surface closer to each other. Initial and boundary conditions for WRF were obtained from the ERA Interim re-analysis data from European Center for Medium Range Weather Forecasts (ECMWF) at 0.7 degree of spatial resolution, which are available every 6 hours (Dee et al. 2011). In this work, we use the WRF model to reproduce the meteorological fields from November 1, 2010 at 12 UTC to November 3, 2010 at 0 UTC. We let WRF run for 9 hours before emission begins so that local circulation could develop. Normally, convective storms develop near 1600 UTC and the peak of activity occurs near sunset.
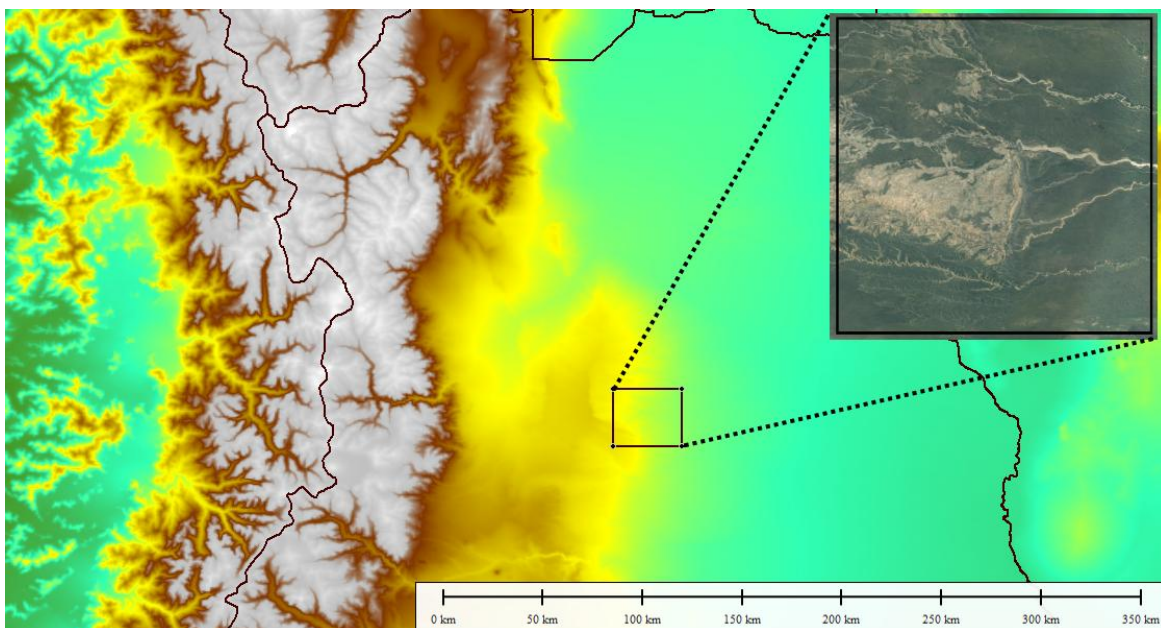

Figure 1: Localization of the simulation domain in the Mendoza Province. Terrain height is color shaded. The generator is located inside the study area, detailed in the LandSat image on the right.

WRF Preprocessing System (WPS)	
Terrain elevation description	Radar Topography Mission (SRTM3) data (Rodriguez et al. 2005)
Land Use and Land Cover (LULC)	Customized (Puliafito et al. 2011)
Physics schemes	
Microphysical scheme	WRF Single Moment 5 class (WSM 5-class)
Long-wave radiative transfer model	Rapid Radiative Transfer Model (RRTM)
Short-wave radiative transfer model	Goddard scheme
Surface physics option	5-layer thermal diffusion
Planet Boundary Layer	No parameterization
Cumulus scheme	Kain-Fritsch scheme

Table 1: WRF physics options used in the simulation. For more details on the physics schemes see Skamarock et al. (2008).

The complex topography in western Argentina requires the use of accurate terrain elevation data for WRF to be able to capture local circulation. The WRF Preprocessing System (WPS) module was modified to include the Shuttle Radar Topography Mission (SRTM3) elevation data (Rodriguez et al. 2005). The standard Land Use/Land Cover (LULC) included in WRF was also replaced by a customized dataset created from the GLOBCOVER 2009 (Arino et al. 2010) Land Cover Map from the European Space Agency (ESA) at a approximately 280 m resolution. This complete set up was previously tested and found to produce the more accurate estimation of temperature, humidity and wind fields at surface and above than any other configuration for the episode simulated (Puliafito et al. 2011). A summary of the model configuration is listed in

WRF Preprocessing System (WPS)	
Terrain elevation description	Radar Topography Mission (SRTM3) data (Rodriguez et al. 2005)
Land Use and Land Cover (LULC)	Customized (Puliafito et al. 2011)
Physics schemes	
Microphysical scheme	WRF Single Moment 5 class (WSM 5-class)
Long-wave radiative transfer model	Rapid Radiative Transfer Model (RRTM)
Short-wave radiative transfer model	Goddard scheme
Surface physics option	5-layer thermal diffusion
Planet Boundary Layer	No parameterization
Cumulus scheme	Kain-Fritsch scheme

Table 1.

2.2 The WRF-Fire model and its adaptation

WRF-Fire (Mandel et al. 2011) combines the Weather Research and Forecasting model (WRF: Skamarock et al. 2008) with a module implementing a surface fire behavior model,

called SFIRE, based on semi-empirical formulas to calculate the rate of spread of the fire line (the interface between burning and unignited fuel) based on fuel properties, wind velocities from WRF, and terrain slope. The heat release from the fire line as well as post-frontal heat release feeds back into WRF dynamics, affecting the simulated weather in the vicinity of the fire (Mandel et al. 2011; Anderson, 1982). Since the fire mesh is generally finer than the atmospheric mesh, wind is interpolated to the nodes of the fire mesh, and the heat flux is aggregated over the cells of the fire mesh that make up one cell of the atmospheric mesh.

In order to estimate the emissions to the atmosphere, WRF-Fire includes a Fire Spread and an Emission Model. Such model uses 13 fuel behavior categories defined by Anderson (1982) to simulate fire spread. For each fuel category there are prescribed properties such fuel mass, depth, density, surface-to-volume ratio, moisture of extinction, and mineral content. There is one additional category to represent "no fuel". In this work, a special fuel category was created to represent the combustion of a ground AgI generator.

In order to run WRF-Fire, ones need to include two additional fields to the static database: fuel map and high resolution terrain elevation data. Both fields should have the resolution of the fire mesh, usually 10 times higher than the meteorological mesh. The best resolution available for terrain elevation is 250 m, from SRTM. The fuel map was created through remapping GLOBCOVER land cover data to match categories in Anderson's fuel categories.

In this work we simulate only one AgI ground generator. It is represented as a small patch in the fuel map, surrounded by an area with no fuel so that fire does not spread beyond that patch. The size of the patch is 60 m by 60 m. Figure 2 shows the fuel map before and after adding the small patch. Figure 3 shows high resolution elevation data.
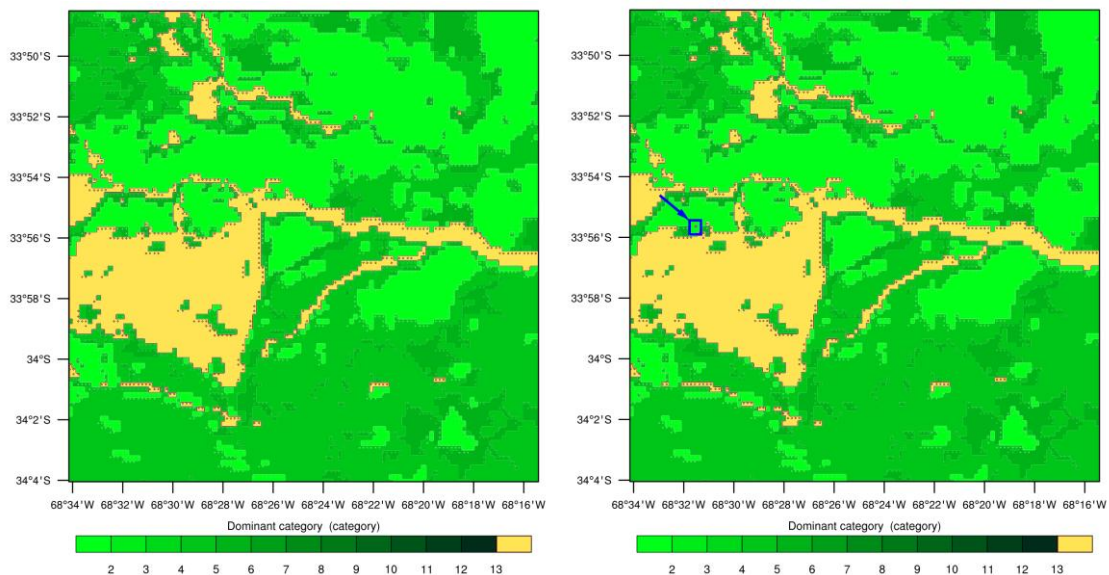

Figure 2: Fuel map before (left) and after (right) adding the small parcel that represents the AgI generator. The color scale represents the 13 Anderson fuel categories. No fuel pixels are in yellow.
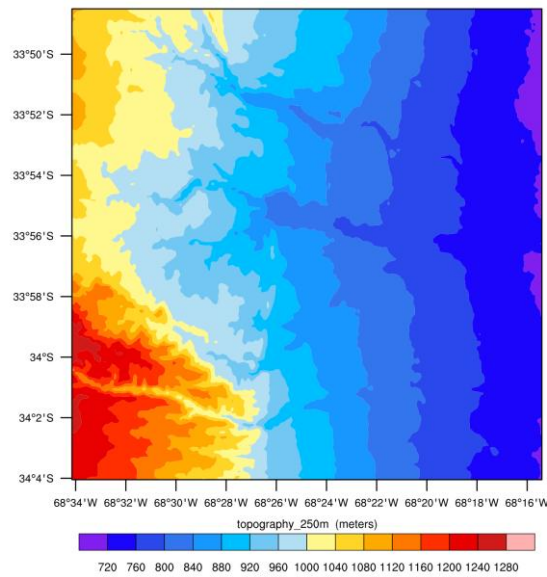
Figure 3: Elevation in meters from the high resolution (250 m) database.

We modified parameters of one of the fuel categories to represent the behavior of the ground generator fuel, a mixture of acetone and silver iodide. We modified the initial mass loading of surface fuel (kg m^{-2}) in order to get fire ignited for 1.5 hours, which is the time ground generator are typically kept on. We also modified the weighting parameter, which determines how long it takes to burn the fuel.

The AgI particles were assumed to have a single mode size distribution and were specified in the model by simulating the release of a tracer. Table 2 shows a summary of parameters for this new fuel model and a summary of relevant model configuration options.

Parameter	Description	Value
fgi	Initial mass loading of fuel (kg m^{-2})	166
weight	Weighting parameter that determines how long it takes to burn fuel	180
fire_ignition_ros	Ignition rate of spread (m/s)	18
fire_ignition_radius	How many nodes will ignite from the center	1

Table 2: Summary of fire model configuration.

2.3 WRF-Fire runs and hardware resources

The model was run on a single machine with a quadruple core, core i7 microprocessor and 16 Gb of RAM. WRF supports parallelism through Open MPI.

In order to meet the Courant-Friedrich-Levy stability criteria, it is recommended that the time step in WRF model be set to less than six times the horizontal grid step (in km) in seconds. In this simulation, the smallest grid step corresponds to the fire grid, which is 0.06 km. The time step chosen is 0.25 seconds.

In each time step of the atmospheric model, the fire module is called from the third step of the Runge-Kutta method in WRF-ARW. With the current setup, each model step takes 0.05 seconds approximately in this system. The whole simulation took 14 hours.

The use of certain microphysics schemes may increase the computational times considerably. As we are not simulating the interaction of AgI with clouds, we choose WRF Single Moment 5 class, which is faster than the more appropriate WRF Single-Moment 6-class scheme, but still useful to predict nucleation process.

3 RESULTS

The impact of the AgI seeding experiments is analyzed in detail in the following sections.

3.1 Validation of the meteorological model

In order to assess how well can the WRF model predict the meteorological conditions during the simulated period, surface observations from 4 agro-meteorological stations were compared to the simulated values. We also test the accuracy of the WRF results by comparing the simulated wind vertical profiles with atmospheric soundings at the Mendoza Airport meteorological station. The characteristics of these stations are shown in Table 3.

Name	Latitude	Longitude	Height (m a.m.s.l.)
Agua Amarga (S)	33° 30' 57,7" S	69° 12' 27" W	970
Altamira (S)	33º 48' 21" S	69º 6' 27.5" W	950
El Peral (S)	33° 20' 48,2" S	69° 9' 27,7" W	1074
Tres Esquinas (S)	33º 52' 08.9" S	69º 5' 16.2" W	850
El Plumerillo (U)	32° 50′ 0″ S	68° 50′ 0″ W	704

Table 3: Agro-meteorological stations (S) and upper air (U) station from the National Weather Service used to validate the model.

Since a consistent procedure should be applied in order to evaluate the model performance, we used the difference between the observed and model-predicted values for 2 m temperature and relative humidity and zonal and meridian wind components. We applied the statistical performance analysis suggested by Willmott (1982). The statistical summary is shown in Table 4. For each pair of modeled and measured values, we calculated the signed difference $(P_i - O_i)$. We computed the mean bias error (MBE), to provide an indication of bias, the root mean square error (RMSE) to show a general indication of the variance. We also included the Willmott's index of agreement (d). Its value goes from 0 to 1.0 for perfect fit.

Station		MBE	RSME	d
Agua Amarga	Temperature	-1.00	2.05	0.96
	Relative Humidity	9.31	12.07	0.82
	U	0.41	2.89	0.57
	V	-0.99	2.20	0.37
Altamira	Temperature	-0.42	3.35	0.92
	Relative Humidity	3.03	9.90	0.89
	U	0.99	3.32	0.49
	V	-0.79	2.66	0.64
El Peral	Temperature	-0.70	2.41	0.95
	Relative Humidity	4.34	9.49	0.90
	U	0.28	2.35	0.82
	V	-0.69	1.72	0.65
Tres Esquinas	Temperature	0.42	3.06	0.94
	Relative Humidity	6.80	10.58	0.85
	U	-0.18	3.83	0.32
	V	-0.48	2.98	0.47

Table 4. Statistical measures of model performance for the four surface stations (U: zonal component of the wind; V:meridional component of the wind) .

The indices of agreement in Table 4 suggest that WRF captured very well the hourly variation of temperature and relative humidity. WRF simulated the wind components acceptably. Relative accuracy was highest for the Altamira and El Peral stations. The low relative accuracy in wind components in the other stations is possibly due to subgrid–scale wind–channeling effects at the observational site. Although the model is unable to reproduce the wind variations exactly, the values of the statistical measures suggest that the system WRF-Fire would produce concentration patterns acceptably.

We also tested the accuracy of the WRF results by comparing the simulated wind vertical profiles with atmospheric soundings at the nearest meteorological station, at the Mendoza Airport. Figure 4 shows, skew-T plots with simulated and measured radiosonde profiles for El Plumerillo station for two simulation days. In most cases, wind prediction accuracy increases with height due to less influence of local terrain effects and more impact of synoptic scale flow patterns on wind speed and direction. For the whole simulation period, mean absolute differences for temperatures are around 1.2 ºC, most being well below this value. Maximum differences are as big as 6.2ºC, though high values seem to happen very seldom as reflected by mean differences being significantly smaller. In general the winds are well reproduced by the model, even near the surface, although the errors observed below 700 hPa are higher.
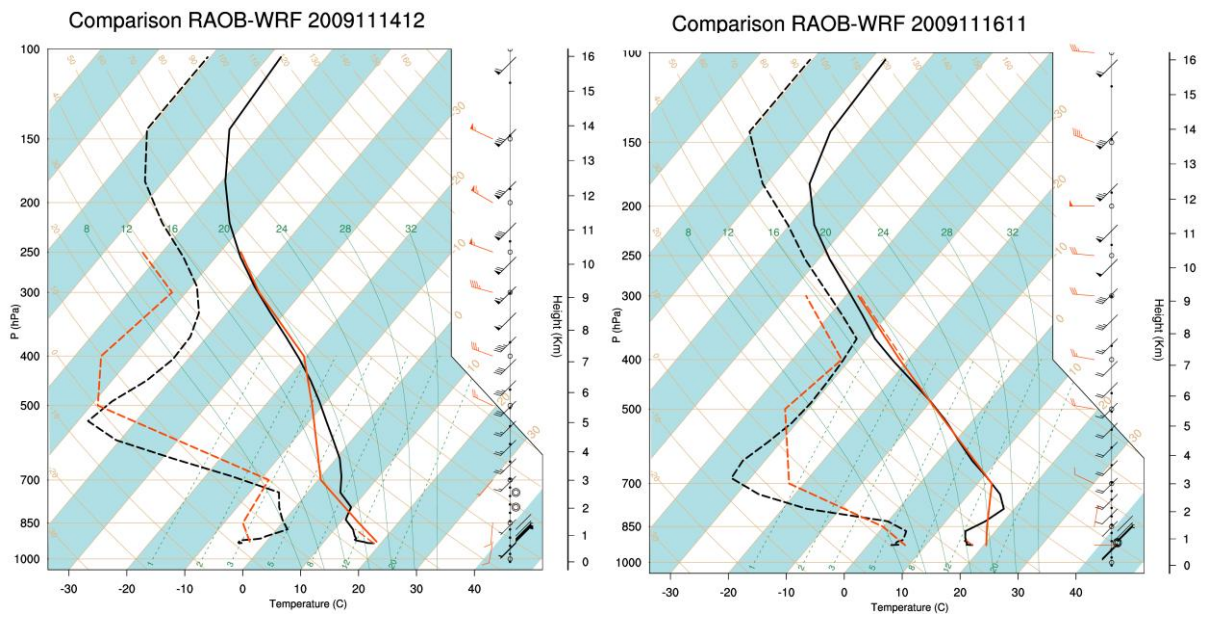
Figure 4. Comparison between WRF outputs (black) and soundings (orange) for two individual measurements in el Plumerillo station, for 11/14/2009 12UTC and 11/16/2009 12 UTC.

Following we show wind roses for a longer simulation period, from November 1th to November 15th, 2009.
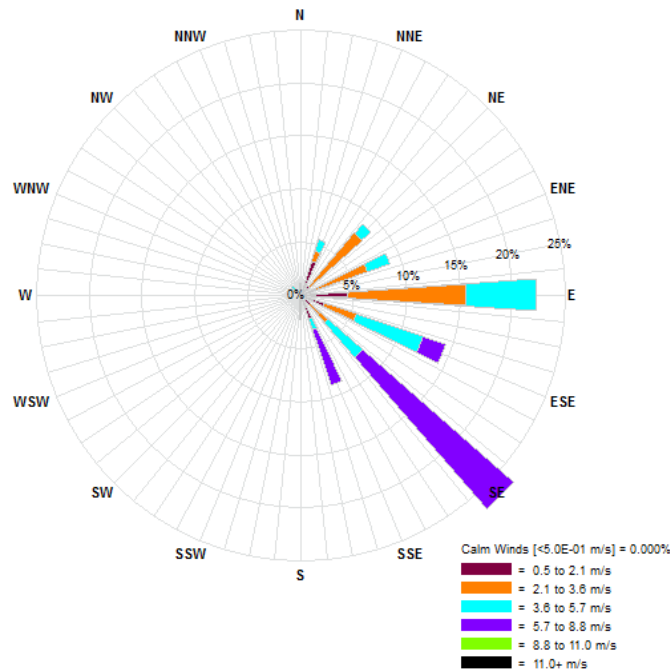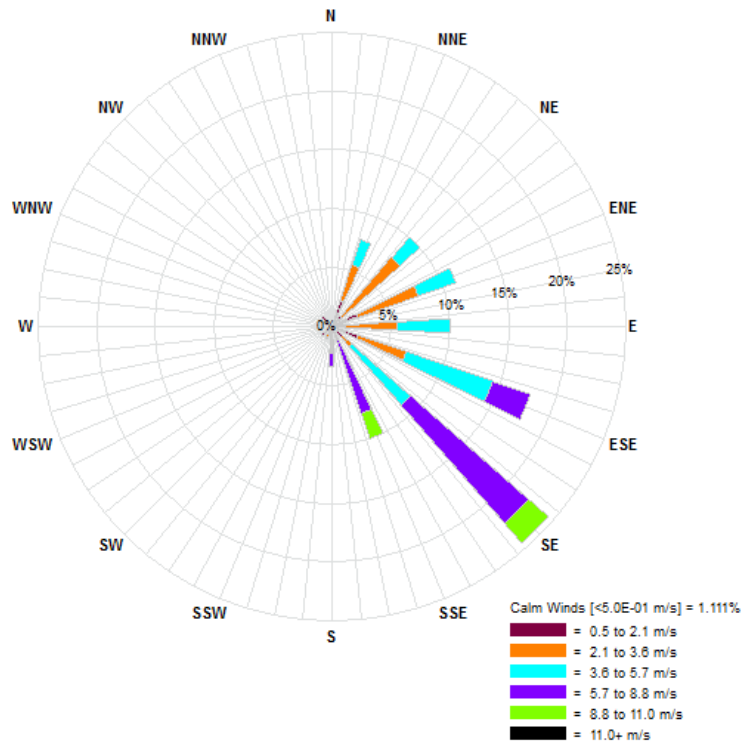

Figure 5. Wind rose at 10 m for a period of time that goes from November 1 to November 21, 2009.

Figure 6. Wind rose at 250 m for a period of time that goes from November 1 to November 21, 2009.
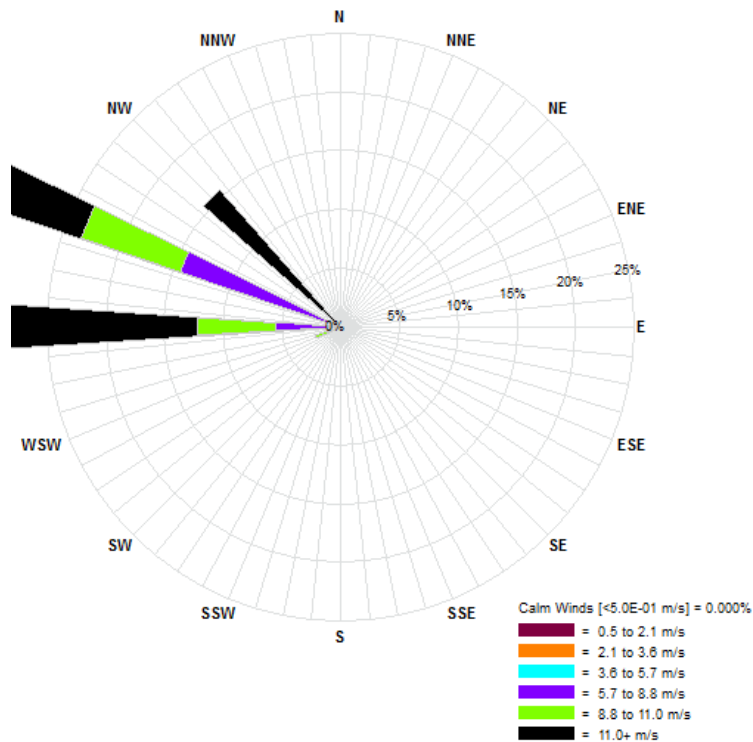

Figure 7. Wind rose at 2500 m for a period of time that goes from November 1 to November 21, 2009.

Wind roses from Figures 5 to 7 show that wind blows mostly from south-east near surface, with speed bellow 6 m/s. On the other hand, at upper levels, with are much stronger, reaching speeds beyond 11 m/s, and it blows mostly from west and north-west. This wind pattern is

also evident in following section where we show dispersion results.

3.2 Dispersion results

Figure 8 shows tracer plume at four different moments: 4, 12, 36 and 72 minutes after ignition.

The series of pictures shows a strong injection of material a few minutes after ignition takes place (first picture). This can be the result of a buoyancy effect due to high fire temperature, and consequently, high emission temperature. The second and third images show the typical valley-mountain circulation. Wind blows uphill at surface level and in the opposite direction at upper levels. The tracer is uplifted by convective wind flow in the region. It is also possible to see how emissions have an effect over local wind. That is due to the coupling mechanism that inputs fire heat flux into the meteorological model.
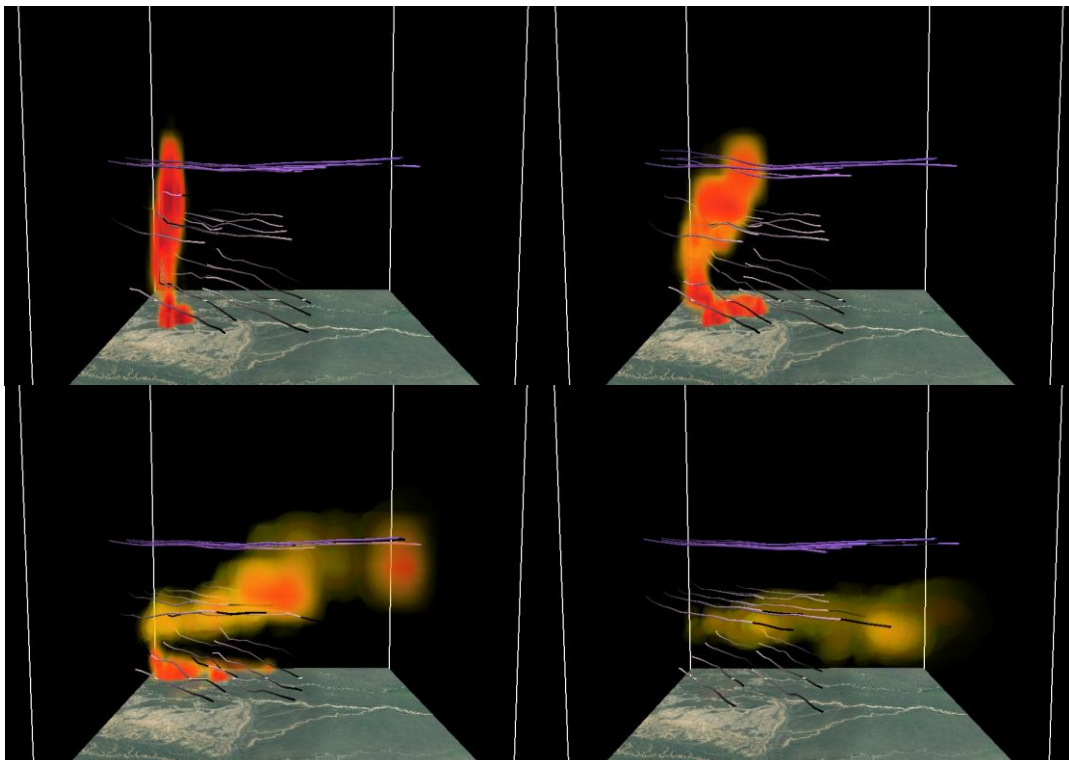

Figure 8. Tracer emission at 4, 12, 36 and 72 minutes after ignition (from left to right and top to botom). Wind pattern is shown at three different levels.

The fourth image shows suspended material after the generator has been turned off.

Figure 9 shows a vertical cross section of the domain in the south-north direction, 1 km away from the source in the east direction, 24 minutes after the emission begins.
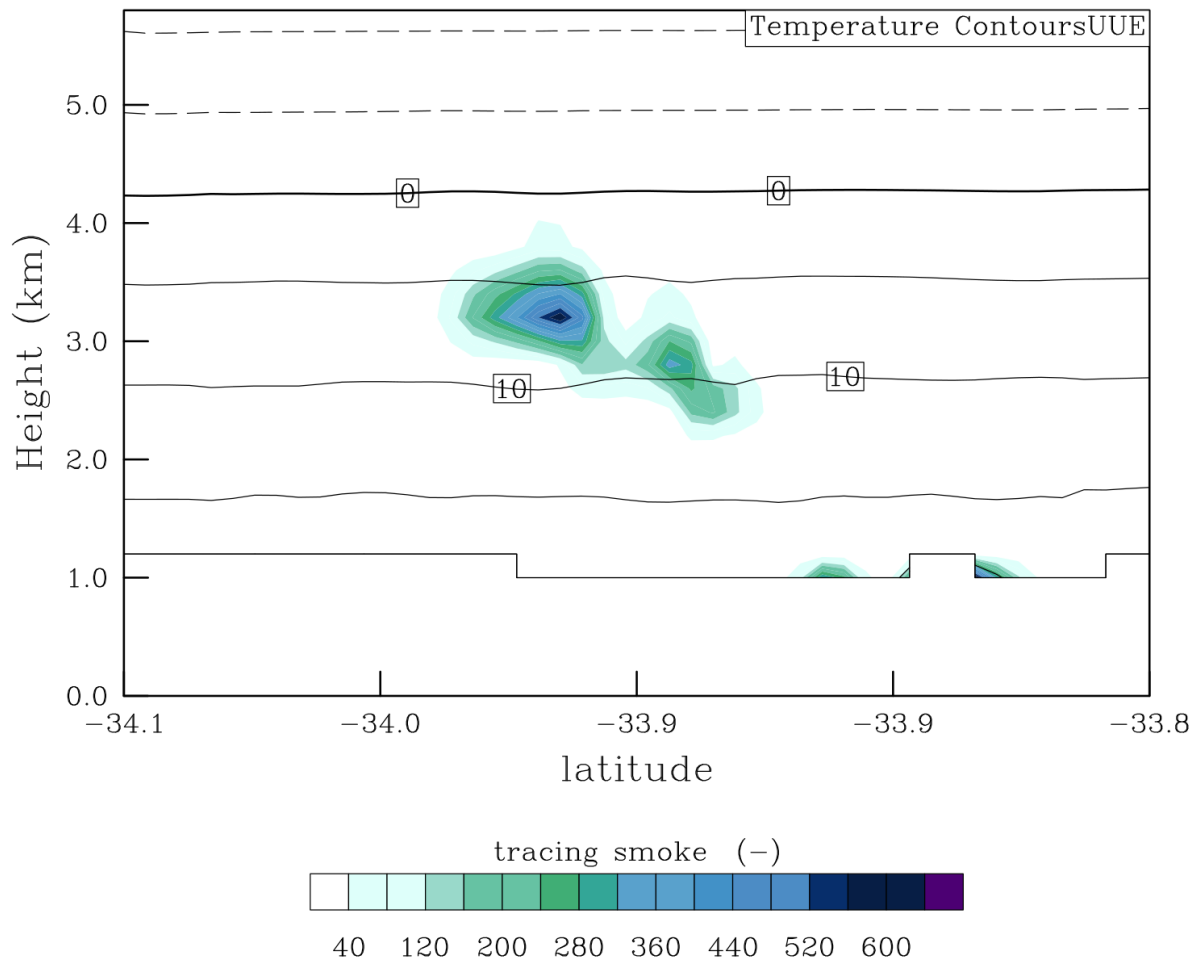
Figure 9. Domain cross-section, 24 minutes after emission begins. The plane cuts the domain 1 km away of the source, in the east direction. Horizontal lines are isotherms. Color contours represent tracer concentration.

The image shows low to moderate concentration of AgI near the surface. The surface wind transports these emissions to the north-east. This near surface concentration of AgI is a point of concern because ground generators are generally placed near cultivated areas where people could be exposed. Furthermore, dry deposition could settle down AgI particles over near rivers.

Figure 10 shows another vertical cross-section in the direction of the plume.
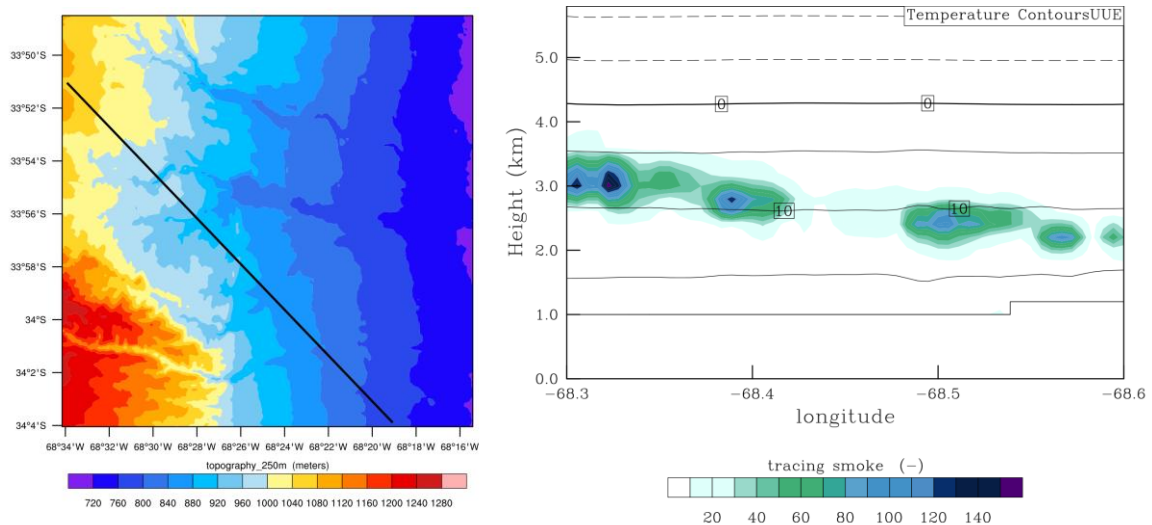
Figure 10. Vertical cross-section of the domain in the direction of the plume. Left panel shows the position of the cutting plane. Right panel show concentration 60 minutes after emission begins.

Simulation results show that emission under this meteorological condition could reach 3.5 km above ground. This altitude is where storm cells generally form, so AgI could be reaching them. In this simulation, wind transport those emissions further south-east, while the target zone is further north. However, under deep convective conditions this situation can change.

4   CONCLUSIONS

This paper shows a possible approach to simulate injection of AgI in storm cells from ground generators used in the hail suppression program in Mendoza. The coupled WRF-Fire model was conceived to simulate fire spread and the local effect that fire emissions can have on meteorology. However, we show how it can also be used to simulate AgI ground generators. The advantage of WRF-Fire over dispersion models like CALPUFF (Scire et al. 2000) is the ability to simulate the atmospheric conditions beyond the Planetary Boundary Layer (PBL), and to simulate the effect of emissions on local meteorology. The method proposed takes advantage of subgrid resolution of the fire model to simulate AgI emission.

The source is modeled as a small parcel through careful modification of one of the 13 fuel behaviors models. This work shows parameters of the fire model that can be modified in order to reproduce the emission profile only. However, we have not tried to simulate emission rate. We are working on the development of a fuel model that could reproduce the emission rate of a real generator. Furthermore, the tracer emission in WRF-Fire has no units, nor any physical property that could be modified to simulate AgI physical properties. Nevertheless, the chemical module of WRF (WRF-Chem) offers 2 chemical mechanisms that could be used to simulate AgI chemistry in the atmosphere. Xue et al. (2013) show efforts to simulate the effects of cloud seeding.

The emission rate in this simulation could be overestimating AgI mass injection at the beginning of the ignition. Moreover, the temperature of such emissions could be modifying local meteorology in an unrealistic manner. However, there are other parameters in the fire model that could help to correct this effect.

According to simulation results, the convective processes that take place during hail storms in the area could take the AgI to the clouds. However, part of the material is transported by near surface wind, and deposited near the source. Such deposition could be of great concern for people living near these sources. This result could be validated with laboratory analysis of

soil and water samples.

In order to be able to simulate with WRF the effect that ground seeding could have on hail suppression, work to be done should include the development of a better way to include sources of AgI emissions and the chemical and physical parameterization of this seeding agent.

5 ACKNOWLEDGMENTS

REFERENCES

Anderson, H.E, Aids to Determining Fuel Models For Estimating Fire Behavior, *USDA Forest Service, Intermountain Forest and Range Experiment Station. General Technical Report INT-122*, 22 pp., 1982.

Arino, O., Ramos, J., Kalogirou, V., Defoumy, P., Achard, F., GlobCover 2009, in: *ESA Living Planet Symposium*. Bergen, Norway, p. 686, 2010.

Browning, K.A., Foote, G.B., Airflow and hail growth in supercell storms and some implications for hail suppression. *Quarterly Journal of the Royal Meteorological Society*, 102(433), pp.499–533, 1976.

Bruintjes, R.T., A Review of Cloud Seeding Experiments to Enhance Precipitation and Some New Prospects. *Bulletin of the American Meteorological Society*, 80(5), pp.805–820, 1999.

Dee, D.P., Uppala, S.M., Simmons, A.J., Berrisford, P., Poli, P., Kobayashi, S., Andrae, U., Balmaseda, M.A., Balsamo, G., Bauer, P., Bechtold, P., Beljaars, A.C.M., van de Berg, L., Bidlot, J., Bormann, N., Delsol, C., Dragani, R., Fuentes, M., Geer, A.J., Haimberger, L., Healy, S.B., Hersbach, H., Hólm, E. V, Isaksen, L., Kållberg, P., Köhler, M., Matricardi, M., McNally, A.P., Monge-Sanz, B.M., Morcrette, J.-J., Park, B.-K., Peubey, C., de Rosnay, P., Tavolato, C., Thépaut, J.-N., Vitart, F., The ERA-Interim reanalysis: configuration and performance of the data assimilation system. *Quarterly Journal of the Royal Meteorological Society* 137, 553–597, 2011.

DeMott, P.J., Quantitative descriptions of ice formation mechanisms of silver iodide-type aerosols. *Atmospheric Research*, 38(1–4), pp.63–99, 1995.

García-Ortega, E., López, L., Sánchez, J.L., Diagnosis and sensitivity study of two severe storm events in the Southeastern Andes. *Atmospheric Research*, 93(1-3), pp.161–178, 2009.

Guo, X., Zheng, G. & Jin, D., A numerical comparison study of cloud seeding by silver iodide and liquid carbon dioxide. *Atmospheric Research*, 79(3–4), pp.183–226, 2006.

Lee, S.S., Donner, L.J. & Phillips, V.T.J., Impacts of aerosol chemical composition on microphysics and precipitation in deep convection. *Atmospheric Research*, 94(2), pp.220–237, 2009.

Li, Z., Pitter, R.L., Numerical Comparison of Two Ice Crystal Formation Mechanisms on Snowfall Enhancement from Ground-Based Aerosol Generators. *Journal of Applied Meteorology*, 36, pp.70–85, 1997.

Makitov, V., Organization and main results of the hail suppression program in the northern area of the province of Mendoza, Argentina. *J. Weather Modif.*, 31, pp.76–86, 1999.

Mandel, J., Beezley, J.D., Kochanski, A. K., Coupled atmosphere-wildland fire modeling with WRF 3.3 and SFIRE 2011. *Geoscientific Model Development*, 4(3), pp.591–610, 2011.

Mezher, R.N., Doyle, M., Barros, V., Climatology of hail in Argentina. *Atmospheric Research*, 114-115, pp.70–82, 2012.

Puliafito, S.E., Allende, D.G., Fernández, R.P., Castro, Fernando Horacio, Cremades, P.G., New Approaches for Urban and Regional Air Pollution Modelling and Management, Nejadkoorki, F. (Ed.), *Advanced Air Pollution,* pp. 429–454, 2011.

Rodriguez, E., Morris, C.S., Belz, J.E., Chapin, E.C., Martin, J.M., Daffer, W., Hensley, S., An assessment of the SRTM topographic products, *Technical Report JPL D-31639*. Pasadena, California, 2005.

Sánchez, J.L., López, L., García-Ortega, E., Gil, B., Nowcasting of kinetic energy of hail precipitation using radar. *Atmospheric Research* 123, 48–60, 2013.

Scire, J.S., Strimaitis, D.G., Yamartino, R.J., *A User's Guide for the CALPUFF Dispersion Model*, 2000.

Silverman, B.A., An evaluation of eleven operational cloud seeding programs in the watersheds of the Sierra Nevada Mountains. *Atmospheric Research*, 97(4), pp.526–539, 2010.

Skamarock, W.C., Klemp, J.B., Gill, D.O., Barker, D.M., Wang, W., Powers, J.G., A Description of the Advanced Research WRF Version 3, Mesoscale and Microscale Meteorology Division, National Center for Atmospheric Research, 2008.

Willmott, C., Some Comments on the Evaluation of Model Performance. *Bulletin of the American Meteorological Society*, 63, pp.1309–1369, 1982.

Xue, L., Tessendorf, S.A., Nelson, E., Rasmussen, R., Breed, D., Parkinson, S., Holbrook, P., Blestrud, D., Implementation of a Silver Iodide Cloud-Seeding Parameterization in WRF. Part II: 3D Simulations of Actual Seeding Events and Sensitivity Tests. *Journal of Applied Meteorology and Climatology*, 52(6), pp.1458–1476, 2013.

Zipori, A., Rosenfeld, D., Shpund, J., Steinberg, D.M., Erel, Y., Targeting and impacts of AgI cloud seeding based on rain chemical composition and cloud top phase characterization. *Atmospheric Research*, 114-115, pp.119–130, 2012.